



DESIGN AND OPTIMIZATION OF LATTICE STRUCTURES FOR AEROSPACE APPLICATIONS

Enrico Stragiotti

François-Xavier Irisarri¹, Cédric Julien¹ and Joseph Morlier²

1: ONERA - The French Aerospace Lab
DMAS - Département matériaux et structures
92320 Châtillon, France
{francois-xavier.irisarri, cedric.julien}@onera.fr

2: ICA - Institut Clément Ader
ISAE - SUPAERO
31400 Toulouse, France
joseph.morlier@isae-supraero.fr
January 22, 2024

PhD manuscript

ONERA – ISAE Supaero

Colophon

This document was typeset with the help of KOMA-Script and L^AT_EX using the kaobook class.

ONERA – ISAE Supaero

CONTENTS

Contents	iii
List of Figures	v
List of Tables	v
List of Abbreviations	v
Abstract	1
Introduction	3
Conclusion and perspectives	7
Appendix	13
A. Sensitivity analysis of the modular structure optimization algorithm	15
A.1. Optimization formulation, objective function and constraints	15
A.2. Common derivatives	16
A.3. Gradient	17
A.4. Jacobian matrix	17
A.5. Hessian matrix	19
Bibliography	21

LIST OF FIGURES

1. (a) The transonic truss-braced wing called ALBATROS by ONERA [1, 2]; (b) the Blended-Wing Body (BWB) zero-e demonstrator by Airbus [3].	3
2. [5] [6].	4

LIST OF TABLES

A.1. Reminder of the indexes used for the sensitivity analysis of the layout and topology optimization of modular structures.	15
---	----

LIST OF ABBREVIATIONS

BWB	Blended-Wing Body
CRM	NASA Common Research Model
DMO	Discrete Material Optimization
DOE	Design of experiments
NAND	Nested Analysis and Design
NLP	Non-Linear Programming
RAMP	Rational Approximation of Material Properties
SAND	Simultaneous Analysis and Design
TTO	Truss Topology Optimization

ABSTRACT

todo

INTRODUCTION

*Scientists study the world as it is,
Engineers create the world that never has been.*

— Theodore von Kármán

TOWARDS LIGHTER STRUCTURES

In the aerospace industry, an ongoing demand exists for lighter aerostructures, motivated by the need to enhance fuel efficiency and overall performance. This emphasis on lighter structures and materials not only reduces operational costs for airlines but also aligns with a broader commitment to sustainability, mitigating fuel consumption and carbon emissions. Furthermore, the aerospace sector is currently witnessing two innovative shifts: the transition to hydrogen-powered and electric planes, directing engineering efforts toward cleaner and more sustainable aviation technologies. These changes offer opportunities to deviate from the classic tube-and-wing configuration and explore inventive concepts like the flying wing Blended-Wing Body (BWB), in which the fuselage and the wing blend together to form an aircraft in which the fuselage, widened and integrated into the wing, also contributes significantly to the lift, or transonic truss-braced wings, with the goal of direct reduction in the aerodynamic drag by using a high-aspect ratio strut-braced wing configuration (see examples in Fig. 1). Regardless of the specific configuration, a highly probable shared goal is the necessity to redesign lightweight dry—i.e. with no fuel tanks inside—wings with high aspect ratios and thin profiles.



(a)



(b)

Figure 1.: (a) The transonic truss-braced wing called ALBATROS by ONERA [1, 2]; (b) the Blended-Wing Body (BWB) zero-e demonstrator by Airbus [3].

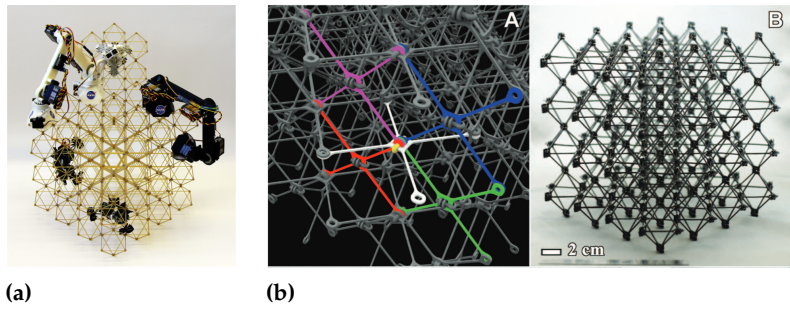


Figure 2.: [5] [6].

4. Belvin et al. (2016), 'In-Space Structural Assembly'

To meet these criteria, a promising solution involves the application of lattice structures. Not only do these structures provide the necessary ultralight properties, but they also offer modularity. Modular designs come with several advantages, notably the capability to construct large structures using smaller, more easily manufactured repeating modules. Other notable properties include on-field reparability, improved damage resistance, fast assembly for temporary structures, and stochastic error detection and repair compared to conventional monolithic material systems [4]. Additionally, recent research opens up the possibility of a fully robotic assembly phase, permitting faster and more reliable assembly (see Fig. 2).

Optimizing lattice structures involves four main dimensions: material, module shape, layout, and topology. Material optimization focuses on improving mechanical properties by tailoring the distribution of lattice constituents, while shape optimization fine-tunes individual module external geometries. Layout optimization arranges modules in space, defining their presence or absence, and topology optimization refines overall arrangement and connections within each module. Navigating these dimensions enables engineers to tailor lattice structures for a balance between weight, strength, and functionality. However, the abundance of design choices poses a significant challenge due to the lack of a standardized design method. Navigating this intricate landscape requires a systematic and efficient approach to ensure the resulting lattice structure meets specific engineering requirements.

OBJECTIVE

This thesis aims to develop an optimization formulation and algorithm specifically designed for ultralight and modular aerostructures within the aerospace industry. In this field, reducing weight is crucial for improving overall performance. However, the introduction of modularity, while offering advantages such as manufacturing easing or improved damage resistance, may potentially lead to an increase in the overall weight of the structure when compared to classic monolithic structures. Consequently, the primary objective throughout this thesis is to develop an optimization method that not only harnesses

the benefits of modularity but also ensures that the resultant structure remains as lightweight as possible. Striking a balance between the manufacturing advantages conferred by modularity and the critical need for weight reduction forms the central focus of this research.

OUTLINE OF THE THESIS

The remainder of the thesis is structured as follows. Chapter ?? provides a comprehensive review of structural optimization algorithms, especially focusing on ultralight weight and modular cases. The chapter introduces density-based topology optimization and the Truss Topology Optimization (TTO) formulations that will be utilized throughout the document. Chapter ?? delves into a detailed comparison of the topology optimization methods, emphasizing results obtained when optimized structures exhibit a very low volume fraction, i.e. less than 5 %. A shared volume minimization with stress constraints formulation is presented, and a comparison is conducted by varying the material mechanical properties to achieve different volume fractions. After careful analysis, the TTO approach is selected due to its reduced computational time and suitability for modeling lightweight structures. Chapter ?? addresses the limitations of the classic TTO formulation, such as the absence of local buckling constraints, minimum slenderness limits, consideration of multiple load cases, and ensuring mechanical compatibility for complex structures. To overcome these challenges, an innovative volume minimization formulation is proposed, incorporating the additional constraints needed to optimize real-world structures. Due to the inherent multimodality of the formulation, a two-step optimization algorithm is introduced, utilizing a relaxed problem to generate an initial approximate solution for subsequent optimization using a complete formulation. The Reinitialization heuristic is also proposed to reduce the influence of the starting point on optimization results. Chapter ?? explores the incorporation of modular constraints in the proposed TTO formulation, employing the full-scale variable linking approach. This approach repeats a single module throughout the entire design to create optimized modular structures. The chapter evaluates the impact of hyperparameters, such as the number of subdomains and module complexity, on the mechanical performance of the structure. A Design of Experiments (Design of experiments (DOE)) based on the chapter's results provides guidance on choosing hyperparameters for optimization. In Chapter ??, the optimization scenario becomes more complex by introducing an additional optimization variable: the addition of multiple different topology modules. This optimization, inherently more complex, involves optimizing not only the modules' topology but also the layout of the modules within the structure. A modified Discrete Material Optimization (DMO) approach is em-

ployed, utilizing a gradient-based optimizer, while the starting point is determined by employing k-means clustering on the stress distribution of the unoptimized initial structure. Up to this point, the focus has been on academic two or three-dimensional test cases. Chapter ?? extends the application of the proposed optimization formulation and algorithms to the aerospace domain. Initially, the monolithic optimization algorithm is used to reduce the weight of the wingbox of the NASA Common Research Model (CRM), a standard benchmark for aeronautic research. The test case is subjected to multiple load cases(+2.5g, -1g and cruise loads) associated with some corresppective safety factors. The optimization is conducted using different materials and discretizations, resulting in lighter structures in less time compared to the literature. Later, the modular optimization formulation presented in Chapter ?? is used on a drone-sized wing based on the 0012 NACA wing profile. Additionally, follow-up scientific perspectives are discussed.

CONCLUSION AND PERSPECTIVES

CONCLUSION

In the aerospace sector, weight reduction plays a fundamental role due to the intricate relationship between weight and lift. In aviation, the need to reduce aircraft weight is essential as it directly influences wing loading, thereby enhancing aerodynamic efficiency, maneuverability, and fuel efficiency. Beyond its economic significance, weight reduction has become a pressing environmental concern. In response to these challenges, innovative concepts such as the BWB or the utilization of transonic truss-braced wings with high elongation have been proposed. These concepts share a common requirement for thin, lightweight wings with a high aspect ratio. A potential design solution fitting well within this context is the application of lattice structures as the primary structure for these wings. The inherent low mass and modular construction benefits make lattice structures an attractive choice. However, the challenge lies in the absence of a standardized method for their design and optimization. Addressing these considerations, this thesis introduces the development of a design method and an optimization algorithm tailored for ultralight lattice structures.

In Chapter ??, we conducted a comprehensive comparison between two optimization frameworks for designing ultralight structures: density-based topology optimization and TTO. Initially, we formulated a shared volume minimization problem with material resistance constraints for both methods. Then, we explored the differences and similarities in their modeling, especially focusing on the disparities between the Nested Analysis and Design (NAND) and Simultaneous Analysis and Design (SAND) approaches. We performed numerical tests using a two-dimensional L-shaped beam as a test case, where we gradually adjusted the material properties to achieve various volume fractions—i.e. high strength is associated with low volume fraction. The results revealed two critical limitations in the applicability of these methods: density-based topology optimization faced challenges at low volume fractions due to the continuous discretization needing mesh refinement, leading to increased computational costs. Conversely, TTO encountered issues at moderately high volume fractions, where the cross-sectional area radius became too large, impacting the truss idealization. Computational time observations highlighted TTO's linear nature, providing clear advantages in this regard. Another important finding is that with continuous discretization, achieving finer details in the optimized structure demands more elements. In contrast, TTO with ground structure discretization eliminates this need, making the optimization process more straightforward and

efficient. Considering these findings, we decided to focus our work on TTO, aligning well with our goal of optimizing ultralight structures.

In Chapter ??, we tackle the main limitations of the TTO method and enhance its applicability. Initially, we introduce a constraint on the minimum slenderness of active bars in optimized structures, expanding the method's range of applicability. We then focus on incorporating local buckling constraints, crucial for lightweight structures, additionally addressing the nodal stability of compressed bars, known as buckling chains or topological buckling. We then model kinematic compatibility constraints to handle more complex scenarios resulting in statically inadmissible structures, such as multiple load cases or imposed symmetries. We formulate the complete TTO approach with these additions, extendable to multiple load cases. However, naively implementing this on a Non-Linear Programming (NLP) solver proves challenging due to the problem's extreme multimodality. To overcome this, we proposed an innovative two-step optimization algorithm. The first step consists of the resolution of a relaxed problem to generate an initial approximate solution for subsequent complete optimization. The reinitialization heuristic reduces the starting point's influence on results. Through this approach, we demonstrate the algorithm's effectiveness on benchmark problems, showcasing its robustness and versatility in handling complex structures under various load cases. Remarkably, in specific case studies like the ten-bar truss, we demonstrated the algorithm's robustness, revealing negligible starting point influence through 100 random initializations. Additionally, when applied to the 2D cantilever beam problem proposed by Achtziger, the algorithm consistently found improved solutions. Furthermore, we extended the testing to more complex scenarios, including a two-dimensional truss subjected to multiple load cases. This highlighted the need to incorporate kinematic constraints into the formulation for accurate optimization. Finally, the algorithm showcased its versatility by successfully optimizing a three-dimensional structure, illustrating its adaptability to diverse engineering challenges.

Chapter ?? is devoted at the implementation of modular constraints in the proposed TTO formulation. Opting for a full-scale method, a method that does not assume physical scale separation between the module and the whole structure, called variable linking, in which the periodicity of the structure is created by linking the design variables of different subdomains of the structure. Mathematically, we enable the consideration of multiple modules' topology by employing the Kronecker product. The subsequent section of the chapter involves a comprehensive examination of the formulation through various numerical optimizations to show the limits and trends of modular TTO optimization. First, we highlight the close relationship between multi-load cases and modular structures, emphasizing the need of kinematic compatibility constraints in modular structures. Then, a

parametric study investigates two key hyperparameters: the number of subdomains and the complexity of the module. Based on the numerical findings, a DOE is constructed, leading to recommendations such as favoring fewer subdomains with modules as large as manufacturably possible. Module complexity, while impacting volume minimization, exhibits a relatively low overall impact. To conclude, the modular TTO structures undergo benchmarking against the widely-used octet-truss lattice.

Modular structures show a mass increase compared to their monolithic counterparts due to the repetition of the same module across the design space, where varying loading conditions may exist. To narrow the gap between modular and monolithic structures, in Chapter ?? we introduce a new design variable: the layout of modules in space. The problem is reformulated to concurrently optimize the topology of multiple modules and their arrangement in the design domain. This task is significantly more challenging due to the strong connection between module topology and layout, compounded by the inherently discrete nature of the layout problem. The discrete design space is firstly relaxed by employing a continuous model and then applying a modified DMO approach with a gradient-based optimizer. To prevent convergence towards non-physical solutions, a dual penalization scheme based on the Rational Approximation of Material Properties (RAMP) method is developed. Finding an appropriate starting point is non-trivial, and we use the k-means clustering approach on the stress distribution of the unoptimized initial structure to provide an initial module layout. The proposed formulation is tested across various two and three-dimensional cases, demonstrating superior results compared to the literature. We show that controlling the number of module topologies and the presence of subdomains effectively reduces the gap between monolithic and modular structures while preserving modular advantages. However, it is essential to note that having more modules is associated with increased manufacturing complexity, and the user must decide the optimal value for their specific application.

In Chapter ??, we extend our analysis to real-world applications from the aerospace domain. Initially, we employ the monolithic optimization algorithm to reduce the weight of the wingbox of the CRM, a standard benchmark in aeronautic research. The test case is subjected to multiple load cases (+2.5g, -1g, and cruise loads) with respective safety factors. The optimization, conducted with various materials and discretizations, results in structures lighter and achieved in less time compared to existing literature. Subsequently, the modular optimization formulation introduced in Chapter ?? is applied to a drone-sized wing based on the 0012 NACA wing profile. This showcases the versatility of the proposed algorithm in addressing complex real-world scenarios and test cases within the aerospace

domain.

PERSPECTIVES

The research opens up various possibilities and potential directions for future exploration. We can categorize these prospects based on the respective chapters.

In Chapter ??, we focused solely on generic density-based topology optimization. It would have been intriguing to compare the results with feature-mapping optimization methods. While we can only speculate, it is likely that the outcomes would not significantly differ since these methods also depend on continuous discretization for finite element analysis and sensitivity analysis. Any variations, especially in terms of computational time, may not be substantial.

Regarding Chapter ??, we primarily addressed local buckling constraints, but it would be valuable to explore the implementation of global buckling constraints. Additionally, we consistently used bar elements instead of beam elements, neglecting the impact of joint stiffness in the optimization. While our assumptions are valid for high slenderness values, it would be interesting to investigate the effects of this switch. Lastly, while multiple mechanical constraints were incorporated into the optimization, the discussion on manufacturing complexity is presented as an outcome of the optimization strategy. It would be essential to consider additional manufacturing constraints, such as a maximum number of bars converging to a single node, or minimum section requirements of the structure during the optimization process.

In Chapter ??, we consistently used cubic modules; however, the external shape of the modules — i.e. the ratio between dimensions or alternative shapes such as pyramidal or dodecahedral — significantly influences the mechanical properties of the module. Investigating this additional design variable in the modular problem is essential, striking a balance between shape complexity, mass, and manufacturing complexity. It's worth noting that numerous studies on the tessellation of 2D and 3D space could serve as inspiration for exploring this direction. Additionally, our focus on topological buckling was limited to within the module, and further exploration on algorithmically implementing topological buckling at the structure level would be intriguing.

Chapter ?? has emphasized the significant challenge of concurrently optimizing the topology and layout of modules. Although the proposed perturbation of the starting point has proven effective in addressing this issue, a more complex heuristic could enhance the optimization process. For instance, an alternating formulation could

be employed, where the layout and topology are optimized sequentially in a repetitive manner until convergence, offering an alternative approach to the intricacies of concurrent optimization.

Finally in Chapter ??, it was observed that the choice of the initial ground structure significantly impacts the optimization of real-sized structures. Extensive studies should be conducted to determine the most effective approach for conceiving the optimal ground structure tailored to specific problems.

APPENDIX

SENSITIVITY ANALYSIS OF THE MODULAR STRUCTURE OPTIMIZATION ALGORITHM

A

In this appendix, we demonstrate how the gradient, Jacobian, and Hessian matrices of the objective function and the optimization constraints are evaluated for the layout and topology optimization formulation \mathbb{M}_2 presented in Chapter ???. This step, called sensitivity analysis, is crucial for gradient descent optimization algorithms, as it allows for faster and more accurate convergence compared to using finite differences. We remind the reader that the index i is relative to the number of bars in a module \bar{n} , the index j is relative to the number of subdomains N_{sub} in which the structure is divided, and the index t is relative to the number of different modules' topologies N_T . The indexes are summarized in Table A.1 for added clarity.

More information on sensitivity analysis can be found in the book by Martins and Ning [7].

A.1. OPTIMIZATION FORMULATION, OBJECTIVE FUNCTION AND CONSTRAINTS

The relaxed formulation \mathbb{M}_2 for which we want to perform the sensitivity analysis is expressed in terms of modules' cross-sectional area \bar{a} , module selection variables α , and member forces q as:

$$\begin{aligned}
 \min_{\bar{a}, \alpha, q} \quad & V = \sum_{j=1}^{N_{\text{sub}}} \bar{\ell}^T \tilde{a}^j \quad (\text{Volume minimization}) \\
 \text{s.t.} \quad & Bq = f \quad (g_{\text{eq}}) \\
 & q \geq -\frac{s\alpha^2}{\ell^2} \quad (g_{\text{buck}}) \\
 & -\sigma_C \alpha \leq q \leq \sigma_T \alpha \quad (g_{\text{st,t}}, g_{\text{st,c}}) \\
 & 0 \leq \bar{a} \leq \frac{4\pi\bar{\ell}^2}{\lambda_{\max}} \quad (g_{\text{slend}}) \\
 & \sum_{t=1}^{N_T} \alpha_t^j \leq 1, \quad \forall j \quad (g_{\text{sum}}),
 \end{aligned} \tag{\mathbb{M}_2}$$

in which

$$V = \sum_{j=1}^{N_{\text{sub}}} \bar{\ell}^T \tilde{a}^j, \tag{A.1}$$

represents the structural volume of the modular structure and acts as the objective function to minimize for the optimization. The vector \tilde{a}^j , representing the increased cross-sectional areas of the j -th subdomain, is defined as follows:

$$\tilde{a}^j = \sum_{t=1}^{N_T} \tilde{w}_t^j \bar{a}_t, \tag{A.2}$$

Index	Interval	Expl.
i	$[0, \bar{n}[$	# of bars in a module
j	$[0, N_{\text{sub}}[$	# of sub- domains # of
t	$[0, N_T[$	modules' topolo- gies

Table A.1.: Reminder of the indexes used for the sensitivity analysis of the layout and topology optimization of modular structures.

and where \tilde{w} is evaluated using the RAMP interpolation scheme with the q parameter as follows:

$$\tilde{w}_t^j = \frac{\alpha_t^j}{1 + q(1 - \alpha_t^j)}. \quad (\text{A.3})$$

The cross-sectional areas vector \mathbf{a}^j of subdomain j used for the constraints evaluation is expressed as:

$$\mathbf{a}^j = \sum_{t=1}^{N_T} w_t^j \bar{\mathbf{a}}_t, \quad (\text{A.4})$$

where $\bar{\mathbf{a}}_t$ represent the vector of cross-sectional areas of the t module and w^j is the vector of weight relatives to the j subdomain, defined as $w^j \in \mathbb{R}^t | w_j^t \in [0, 1]$. Its relationship with the weight w is as follows:

$$w_t^j = \frac{\alpha_t^j}{1 + p(1 - \alpha_t^j)}, \quad (\text{A.5})$$

where $p \in \mathbb{R}^+$ denotes a parameter governing the steepness of the RAMP interpolation.

A.2. COMMON DERIVATIVES

We introduce here some important derivatives that we use all along the Chapter.

$$\frac{\partial \mathbf{a}^j}{\partial \bar{\mathbf{a}}_t} = w_t^j, \quad (\text{A.6})$$

$$\frac{\partial \mathbf{a}^j}{\partial \alpha_t^j} = \frac{\partial \mathbf{a}^j}{\partial w_t^j} \frac{\partial w_t^j}{\partial \alpha_t^j}, \quad (\text{A.7})$$

where

$$\frac{\partial \mathbf{a}^j}{\partial w_t^j} = \bar{\mathbf{a}}_t, \quad (\text{A.8})$$

and

$$\frac{\partial w_t^j}{\partial \alpha_t^j} = \frac{1 + (\cdot)}{\left(1 + (\cdot)(1 - \alpha_t^j)\right)^2}, \quad (\text{A.9})$$

where (\cdot) is either equal to p or q .

$$\frac{\partial^2 w_t^j}{\partial (\alpha_t^j)^2} = \frac{2(\cdot)(1 + (\cdot))}{\left(1 + (\cdot)(1 - \alpha_t^j)\right)^3}. \quad (\text{A.10})$$

A.3. GRADIENT

The gradient of the objective function V is non-zero only for the design variables $\bar{\alpha}$ and α . It is evaluated for $\bar{\alpha}$ as following:

$$\frac{\partial V}{\partial \bar{\alpha}_t} = \bar{\ell}^T \sum_{j=1}^{N_{\text{sub}}} \tilde{w}_t^j, \text{ with } t \in [1, \dots, N_T]. \quad (\text{A.11})$$

The gradient with respect to α can be written as:

$$\frac{\partial V}{\partial \alpha_t^j} = \frac{\partial V}{\partial w_t^j} \frac{\partial w_t^j}{\partial \alpha_t^j}, \quad (\text{A.12})$$

where

$$\frac{\partial V}{\partial w_t^j} = \bar{\ell}^T \bar{\alpha}_t, \quad (\text{A.13})$$

and evaluated using Equation A.9 and the parameter q . As already mentioned, the gradient is zero with respect to the member forces q :

$$\frac{\partial V}{\partial q} = 0. \quad (\text{A.14})$$

A.4. JACOBIAN MATRIX

We focus now on the evaluation of the Jacobian matrix of the optimization constraints with respect to the design variables.

EQUILIBRIUM CONSTRAINTS The equilibrium constraint g_{eq} is linear on q and not dependent on $\bar{\alpha}$ and α . For that reason we can write:

$$\frac{\partial g_{\text{eq}}}{\partial \bar{\alpha}} = 0, \quad (\text{A.15})$$

$$\frac{\partial g_{\text{eq}}}{\partial \alpha} = 0, \quad (\text{A.16})$$

$$\frac{\partial g_{\text{eq}}}{\partial q} = B. \quad (\text{A.17})$$

STRESS CONSTRAINTS Knowing that:

$$\frac{\partial g_{\text{st,t}}^j}{\partial \alpha^j} = -\sigma_t, \quad (\text{A.18})$$

and

$$\frac{\partial g_{\text{st,c}}^j}{\partial \alpha^j} = \sigma_c, \quad (\text{A.19})$$

the Jacobian for the stress constraints $g_{st,t}$ and $g_{st,c}$ can be evaluated using Equation A.6 and Equation A.7 as follows:

$$\frac{\partial g_{st,*}^j}{\partial \bar{a}_t} = \frac{\partial g_{st,*}^j}{\partial \alpha^j} \frac{\partial \alpha^j}{\partial \bar{a}_t}, \quad (\text{A.20})$$

and

$$\frac{\partial g_{st,*}^j}{\partial \alpha^j} = \frac{\partial g_{st,*}^j}{\partial \alpha^j} \frac{\partial \alpha^j}{\partial \alpha^j}, \quad (\text{A.21})$$

where the asterisk * refers to either the compression and the tension constraints. The stress constraints are linear with respect to q :

$$\frac{\partial g_{st,*}}{\partial q} = \mathbf{1}, \quad (\text{A.22})$$

in which $\mathbf{1}$ represent a vector of all ones.

BUCKLING CONSTRAINTS Knowing that:

$$\frac{\partial g_{buck}^j}{\partial \alpha^j} = 2 \frac{s \alpha^j}{\ell^2}, \quad (\text{A.23})$$

the Jacobian for the buckling constraints g_{buck} with respect to \bar{a} can be evaluated using Equation A.6 as:

$$\frac{\partial g_{buck}^j}{\partial \bar{a}_t} = \frac{\partial g_{buck}^j}{\partial \alpha^j} \frac{\partial \alpha^j}{\partial \bar{a}_t}. \quad (\text{A.24})$$

Using Equation A.7 we evaluate the derivative with respect to α as:

$$\frac{\partial g_{buck}^j}{\partial \alpha^j} = \frac{\partial g_{buck}^j}{\partial \alpha^j} \frac{\partial \alpha^j}{\partial \alpha^j}. \quad (\text{A.25})$$

MAXIMUM SUM ALPHA CONSTRAINTS The constraint g_{sum} on the maximal value of α in every subdomain is linear with respect to α and it does not depend on the other design variables. For that reason we can write:

$$\frac{\partial g_{sum}}{\partial \bar{a}} = 0, \quad (\text{A.26})$$

$$\frac{\partial g_{sum}}{\partial \alpha} = \mathbf{1}, \quad (\text{A.27})$$

$$\frac{\partial g_{sum}}{\partial q} = 0. \quad (\text{A.28})$$

A.5. HESSIAN MATRIX

For the evaluation of the hessian matrix, we list here only the nonzero contributions, assuming that all the remaining are zero.

VOLUME The only nonzero contributions to the Hessian matrix are:

$$\frac{\partial^2 V}{\partial \bar{a}_t \partial \alpha_t^j} = \bar{\ell}^T \frac{\partial \tilde{w}_t^j}{\partial \alpha_t^j}, \quad (\text{A.29})$$

and

$$\frac{\partial^2 V}{\partial (\alpha_t^j)^2} = \bar{\ell}^T \bar{a}_t \frac{\partial^2 w_t^j}{\partial (\alpha_t^j)^2}, \quad (\text{A.30})$$

that can be evaluated using Equation A.9 and Equation A.10

EQUILIBRIUM CONSTRAINTS All terms are zero for the equilibrium constraints.

STRESS CONSTRAINTS

$$\frac{\partial^2 g_t^j}{\partial \bar{a}_t \partial \alpha_t^j} = -\sigma_t \frac{\partial w_t^j}{\partial \alpha_t^j}, \quad (\text{A.31})$$

$$\frac{\partial^2 g_t^j}{\partial (\alpha_t^j)^2} = -\sigma_t \bar{a}_t \frac{\partial^2 w_t^j}{\partial (\alpha_t^j)^2}. \quad (\text{A.32})$$

BUCKLING CONSTRAINTS To evaluate the Hessian of buckling constraints we need to define two additional indexes, l and m that are spanning from 0 to $N_T - 1$ as the index t . We can then write:

$$\frac{\partial^2 g_{\text{buck}}^j}{\partial \bar{a}_l \partial \bar{a}_m} = 2 \frac{s}{\ell^2} w_l^j w_m^j. \quad (\text{A.33})$$

The mixed term is evaluated as follow:

$$\frac{\partial^2 g_{\text{buck}}^j}{\partial \bar{a}_l \partial \alpha_m^j} = 2 \frac{s}{\ell^2} w_l^j \frac{\partial a^j}{\partial \alpha_m^j} + 2 \frac{s a^j}{\ell^2} \frac{\partial w_l^j}{\partial \alpha_m^j}, \quad (\text{A.34})$$

$$\frac{\partial^2 g_{\text{buck}}^j}{\partial \bar{a}_l \partial \alpha_m^j} = 2 \frac{s}{\ell^2} w_l^j \frac{\partial w_m^j}{\partial \alpha_m^j} \bar{a}_m + 2 \frac{s a^j}{\ell^2} \frac{\partial w_l^j}{\partial \alpha_m^j}, \quad (\text{A.35})$$

$$\frac{\partial^2 g_{\text{buck}}^j}{\partial \bar{a}_l \partial \alpha_m^j} = \begin{cases} 2 \frac{s}{\ell^2} \frac{\partial w_t^j}{\partial \alpha_t^j} (w_t^j \bar{a}_t + a^j) & \text{if } l = m = t \\ 2 \frac{s}{\ell^2} w_l^j \frac{\partial w_m^j}{\partial \alpha_m^j} \bar{a}_m & \text{otherwise.} \end{cases} \quad (\text{A.36})$$

And finally the quadratic term in α :

$$\frac{\partial^2 g_{\text{buck}}^j}{\partial \alpha_l^j \partial \alpha_m^j} = 2 \frac{s}{\ell^2} \bar{a}_l \frac{\partial a^j}{\partial \alpha_m^j} \frac{\partial w_l^j}{\partial \alpha_l^j} + 2 \frac{s a^j}{\ell^2} \bar{a}_l \frac{\partial^2 w_l^j}{\partial \alpha_l^j \partial \alpha_m^j}, \quad (\text{A.37})$$

$$\frac{\partial^2 g_{\text{buck}}^j}{\partial \alpha_l^j \partial \alpha_m^j} = \begin{cases} 2 \frac{s}{\ell^2} \bar{a}_t^2 \left(\frac{\partial w_t^j}{\partial \alpha_t^j} \right)^2 + 2 \frac{s a^j}{\ell^2} \bar{a}_t \frac{\partial^2 w_t^j}{\partial (\alpha_t^j)^2} & \text{if } l = m = t \\ 2 \frac{s}{\ell^2} \bar{a}_l \bar{a}_m \left(\frac{\partial w_m^j}{\partial \alpha_m^j} \right) \left(\frac{\partial w_l^j}{\partial \alpha_l^j} \right) & \text{otherwise.} \end{cases} \quad (\text{A.38})$$

MAXIMUM SUM ALPHA CONSTRAINTS All terms are zero for the g_{sum} constraint.

BIBLIOGRAPHY

- [1] Carrier, G., Atinault, O., Dequand, S., and Toussaint, C., 'Investigation of a Strut-Braced Wing Configuration for Future Commercial Transport', 2012, p. 16. cited on page 3
- [2] Carrier, G. G., Arnoult, G., Fabbiane, N., Schotte, J.-S., David, C., Defoort, S., Benard, E., and Delavenne, M., 'Multidisciplinary analysis and design of strut-braced wing concept for medium range aircraft', *AIAA SCITECH 2022 Forum*, AIAA SciTech Forum, American Institute of Aeronautics and Astronautics, Dec. 2021.
doi: [10.2514/6.2022-0726](https://doi.org/10.2514/6.2022-0726) cited on page 3
- [3] Airbus, 'Airbus reveals new zero-emission concept aircraft | Airbus', Oct. 2021.
URL: <https://www.airbus.com/en/newsroom/press-releases/2020-09-airbus-reveals-new-zero-emission-concept-aircraft> cited on page 3
- [4] Belvin, W. K., Doggett, W. R., Watson, J. J., Dorsey, J. T., Warren, J. E., Jones, T. C., Komendera, E. E., Mann, T., and Bowman, L. M., 'In-Space Structural Assembly: Applications and Technology', *3rd AIAA Spacecraft Structures Conference*, AIAA SciTech Forum, American Institute of Aeronautics and Astronautics, Jan. 2016.
doi: [10.2514/6.2016-2163](https://doi.org/10.2514/6.2016-2163) cited on page 4
- [5] Cheung, K. C. and Gershenfeld, N., 'Reversibly Assembled Cellular Composite Materials', *Science* 341.6151 (Sept. 2013), Publisher: American Association for the Advancement of Science Section: Report, pp. 1219–1221.
doi: [10.1126/science.1240889](https://doi.org/10.1126/science.1240889) cited on page 4
- [6] Costa, A., Jenett, B., Kostitsyna, I., Abdel-Rahman, A., Gershenfeld, N., and Cheung, K., 'Algorithmic Approaches to Reconfigurable Assembly Systems', *arXiv:2008.11925 [cs]* (Aug. 2020), arXiv: 2008.11925.
doi: [10.1109/AERO.2019.8741572](https://doi.org/10.1109/AERO.2019.8741572) cited on page 4
- [7] Martins, J. and Ning, A., 'Engineering Design Optimization'. Cambridge University Press, 2021.
ISBN: [978-1-108-83341-7](https://doi.org/10.108-83341-7) cited on page 15

